Synthesis and Characterization of Zeolite L

Yong Sig Ko and Wha Seung Ahn*

Department of Industrial Chemistry, Sinsung Junior College, Dangjin-gun 343860, Korea
Department of Chemical Engineering, College of Engineering, Inha University, Inchon 402751, Korea
Received December 8, 1998

Substantial reduction in synthesis time was achieved for zeolite L crystallization by attempting a hydrothermal synthesis at elevated temperature of 443K in a Na/K mixed alkali system. Pure zeolite L could be obtained from a gel with the molar composition $5.4K_2O$-$5.7Na_2O$-Al_2O_3-$30SiO_2$-$500H_2O$ after 24h. Zeolite L could be obtained in high purity at the optimum $Na_2O/(K_2O+Na_2O)$ ratio of around 0.5 whilst zeolite W was formed when the $Na_2O/(K_2O+Na_2O)$ ratio was more than 0.66. The crystalline zeolite L samples obtained were characterized by means of elemental chemical analysis, XRD, SEM, FTi.r. spectroscopy, and particle size analyzer. In addition, two probe reaction studies were conducted. In toluene alkylation, H-L catalyst showed high catalytic activity at the beginning, but was deactivated quickly probably due to one-dimensional pore sturcture being blocked by the coke formed. High amounts of trimethylbenzene or diethylbenzene were observed due to the large 12-membered ring pore structure of zeolite L. Pt/NaKL catalyst prepared showed a high conversion of n-hexane and high selectivity to benzene in n-hexane aromatization reaction.

Introduction

The crystal structure of zeolite L was determined initially by Barrer and Villiger.[1] The zeolite L has one-dimensional pores of about 0.71nm aperture leading to cavities of about 0.48×1.24×1.07 nm and its Si/Al ratio is typically 3.0.[2] Preparations of the zeolite L have been reported mostly as patents by various investigators,[3~7] with or without using an organic templates, claiming different morphologies. Some investigations have studied on the properties of L-type zeolite with regards to its structure,[1,2] adsorptive properties[8,9] and catalytic properties.[10] Especially zeolite L, due to its unique structural features, is known as a good support for a catalyst used in aromatization of the C_6-hydrocarbons of normal structure[11] and is being used commercially in the Chevron Aromax cyclization process[12]; A monofunctional catalyst consisting of platinum on the non-acidic zeolite L has been reported to have high catalytic activity and high selectivity to benzene for conversion of n-hexane.[13,14]

Most of the studies dealing with zeolite L synthesis so far have been conducted at relatively low temperatures ranging from 273 to 403 K in a K^+ ionic system, and usually it took 3 to 10 days to obtain a highly crystalline product. Furthermore, careful control of the substrate mixture composition was a prerequisite to avoid coprecipitation of undesirable zeolite W or T phases. In this work, a new attempt was made to prepare zeolite L at substantially higher temperature of 443 K in a Na^+/K^+ mixed alkali system to accelerate the crystallization process. Much efforts were given to verify the optimum substrate composition to obtain high purity zeolite L crystals. In particular, the effect of the ionic ratios in the mixed alkali system on zeolite L synthesis was examined closely. To evaluate the quality of the product obtained, a detailed investigation on the physico-chemical properties of the zeolite L prepared was conducted as well as probe reaction studies. For the latter purpose, toluene alkylation with ethanol and n-hexane aromatization after dry-impregnation of a Pt precursor was briefly examined.

Experimental

Synthesis. Zeolite L synthesis was attempted from substrates having the following composition range expressed as oxide mole ratios: SiO_2/Al_2O_3=10-35, $(K_2O+Na_2O)/SiO_2$ =0.30-0.55, $Na_2O/(K_2O+Na_2O)$=0.20-0.68, $H_2O/(K_2O+Na_2O)$=30-60. Colloidal silica sol (Ludox HS-40 from Dupont, 40% SiO_2) and Sodium aluminate (Junsei Co., 32.6% Na_2O, 35.7% Al_2O_3) were used as a source of silica and alumina, respectively. Potassium hydroxide (Tedia Co., 85%) and sodium hydroxide (Tedia Co., 98%) were used for alkali metal cations. Calculated amounts of sodium hydroxide, potassium hydroxide and alumina source were added to the deionized water to prepare a sodium and potassium aluminate solution in a teflon reaction vessel (100 mL) and stirred until the alumina source was dissolved. This solution was then added slowly to the calculated amount of aqueous silica solution and the whole mixture was stirred vigorously for 30 minutes for homogenization. The reaction mixture was transferred to a 100 mL teflon-lined stainless steel autoclave and maintained in the air-heated oven at 443 K under static conditions. Autoclaves were removed from the oven at the schedued times and were quenched in cold water for product identification. The solid products were separated by filtration. Excess alkali were washed with deionized water repeatedly until the pH of washing liquid was close to 9, and the products were dried in an oven at 393 K for 12h.

Characterization. The synthesized samples were analyzed by X-ray diffraction (XRD) for phase identification. The unit used was a powder X-ray diffractometer (Philips, PW-1700) with a scintillation counter and a graphite mono-

*To whom correspondence should be addressed.

chromator attachment, utilizing Ni-filtered CuKα radiation. To calculate crystallinity, peaks located at 2θ=5.5, 19.4, 22.7, 28.0, 29.1 and 30.7 were used to avoid the possible interference of the coexisting other phases such as W or T for a given sample. The morphology of the crystalline phase was examined using a scanning electron microscope (Hitachi, X-650) after coating with an Au-Pd evaporated film. FT-IR spectra of the samples were recorded in air at room temperature using a Perkin-Elmer series 2000 spectrometer (in the range of 400-4000 cm^{-1}) with wafers of zeolites mixed with dry KBr. The average crystal size and particle size distribution were measured with a dynamic scattering particle size analyzer (Malvern, Zetasizer 4). In order to avoid counting amorphous gel particles, the gel was treated in 1.5 M NaOH solution for 1h. Thermogravimetric and differential thermal analysis were performed on a Dupont 2000 thermal analyzer in the temperature range 298-1073 K with 20 mg sample, at a heating rate of 10K min^{-1} and in the air stream of 7 *l*/h. Finely powdered and calcined alumina was used as a reference sample. The specific surface areas and micropore volumes were determined by nitrogen physisorption with the BET method at liquid nitrogen temperature using a Micromeritics ASAP 2000 automatic analyzer. The chemical analysis of the crystalline samples was performed using ICP (Jobin Yuon JY-38 VHR) and XRF (Rigaku, 3070).

Catalytic reaction study. The H-forms of the zeolites were obtained by ion-exchanging. The ion-exchange process was repeated 3 times using 1M ammonium nitrate aqueous solution at 369 K for 19h. The ion-exchanged sample was washed until no nitrate ion were detected, and dried at 373 K during overnight and calcined at 773 K for 3h. Toluene alkylation with ethanol was carried at atmospheric pressure at 623 K in a conventional fixed bed microreactor using the 0.1 g H-form catalyst pretreated in hydrogen for 2h at 773 K. The liquid mixture (2 : 1 molar ratio) of toluene/ethanol was fed to the evaporator using a syringe pump. The carrier gas, H_2, transported the liquid mixture to the microreactor. The reaction products were analyzed by on-line GC equipped with 4.5 m column packed with 5% Bentone-34 and 5% diisodecyl phthalate on Uniport B.

2 wt% Pt/KNaL catalysts were prepared by the incipient wetness impregnation using an aqueous solution of $Pt(NH_3)_4Cl_2$. Theses were dried at 383 K and then activated in flowing oxygen by linear heating to 593 K for 12h and maintaining at this temperature for 2h. n-Hexane aromatization was carried out under atmospheric pressure at 773 K in a conventional fixed bed microreactor with 0.2 g catalyst pretreated in hydrogen for 6h at 803 K. The hydrogen/n-hexane ratio was fixed at 6 and the contact time was 2.6s. The reaction products were analyzed by GC equipped with flame ionization detector using Porapak-Q and SE-30 columns.

Results and Discussion

The influence of hydrothermal synthesis temperature on zeolite L crystallization process was examined, initially. Figure 1 shows the crystallization curves of zeolite L synthesized at different reaction temperatures from a substrate of composition $5.4K_2O$-$5.7Na_2O$-Al_2O_3-$30SiO_2$-$500H_2O$. It was observed that the increase in reaction temperature caused a decrease in the induction period and shortening the overall crystallization period. This result suggests that the rate of nucleation has been accelerated with the increase of reaction temperature. For the zeolite L samples obtained at the reaction temperature of 373 K, the maximum crystallinity of the zeolite phase reached only to 48% even after 7 days. On the other hand, highly crystalline zeolite L crystals

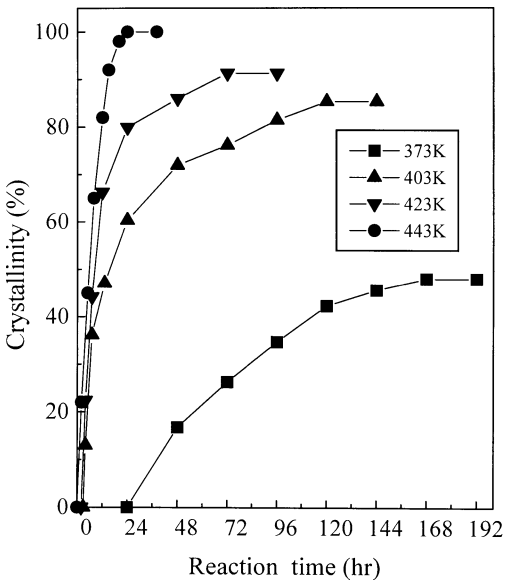

Figure 1. Effect of reaction temperature on the crystallization of zeolite L from the substrate composition of $5.4K_2O$-$5.7Na_2O$-Al_2O_3-$30SiO_2$-$500H_2O$.

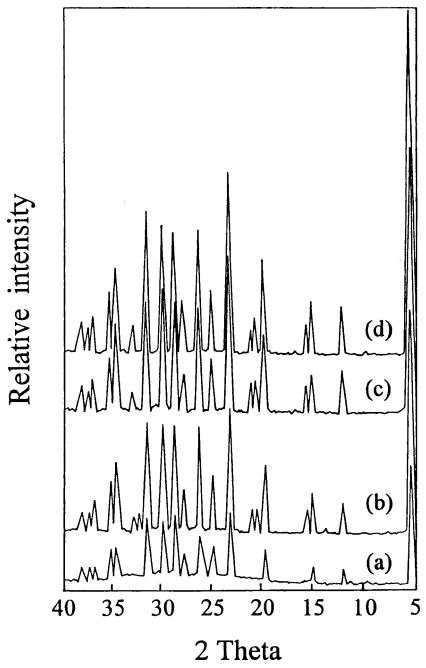

Figure 2. X-ray diffraction patterns of zeolite L samples obtained with different crystallization periods at 443 K. Substrate composition: $5.4K_2O$-$5.7Na_2O$-Al_2O_3-$30SiO_2$-$500H_2O$; (a) 4 h, (b) 12 h, (c) 20 h, and (d) 24 h.

were obtained in 24h at 443 K. Subsequently, zeolite L crystallization process was more closely examined as a function of synthesis time at 443 K. Figure 2 shows the X-ray diffraction patterns of the zeolite L samples obtained at different crystallization periods. The peak intensities developed progressively as the crystallization period increased. Characteristic XRD peaks of the zeolite L began to appear after 4h at 443K, and the fully crystalline zeolite L sample was obtained after 24h. No other crystalline phases appeared in the XRD pattern of this sample even after the prolonged crystallization period up to 72h. The corresponding SEM photographs of zeolite L samples are shown in Figure 3. Amorphous material gradually disappeared as the crystallization progressed, and the amount of crystalline zeolite L phase increased. After 12h amorphous material disappeared completely and typical clam shaped crystals of domed basal plane with the mean diameter of 1.4 μm resulted. The particle size distributions depending on the crystallization periods are shown in Figure 4. The average crystal sizes at the synthesis periods of 12, 20 and 24h were 0.3, 1.2 and 1.4 μm, respectively, and the particle size distribution gradually became broader and approached an asymptotic value as the crystallization time increased.

The crystallinity of a particular desired zeolite phase can also be improved by the choice and amount of inorganic cation used in the synthesis gel. It is known that K^+ ion is necessary for the crystallization of pure zeolite L, because its framework structure is based on the cancrinite cage occupied by K^+ ion.[15] However, the crystallinity of the zeolite L can be improved with the addition of sodium ions to the synthesis gel. Sodium replacement of potassium ions, which is given by the $Na_2O/(K_2O+Na_2O)$ in the reaction mixture under the same SiO_2/Al_2O_3, $(K_2O+Na_2O)/SiO_2$ and $H_2O/(K_2O+Na_2O)$ ratio, was found to affect both the degree of crystallization and the morphology of the product crystals. Figure 5 shows the effect of $Na_2O/(K_2O+Na_2O)$ ratios of synthesis mixture on the zeolite L crystallization at constant ratios of SiO_2/Al_2O_3, $(K_2O+Na_2O)/SiO_2$ and $H_2O/(K_2O+Na_2O)$. A sharp increase in crystallinity was observed with increasing $Na_2O/(K_2O+Na_2O)$ ratio, until the ratio in

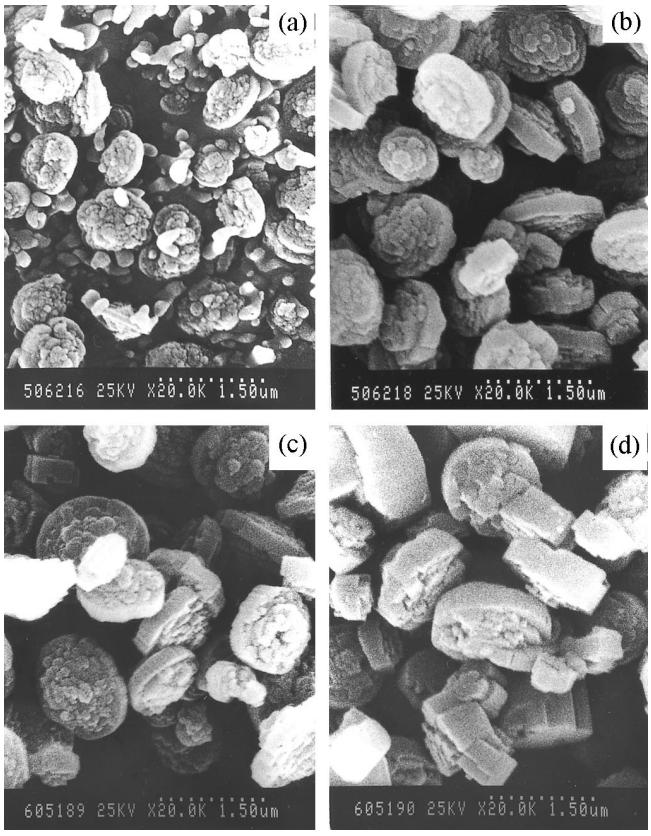

Figure 3. SEM photographs of zeolite L crystals obtained with different crystallization periods at 443 K. (a) 4 h, (b) 12 h, (c) 20 h, and (d) 24 h.

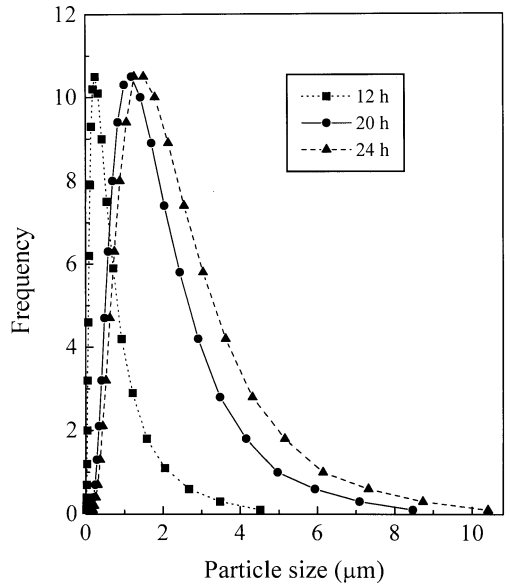

Figure 4. Particle size distribution of zeolite L synthesized with different crystallization periods at 443 K.

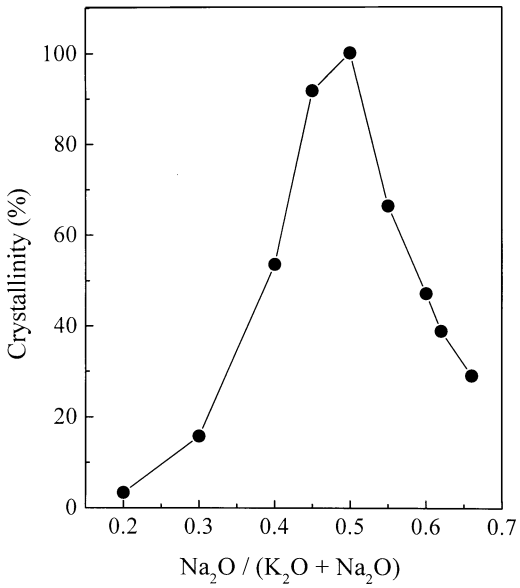

Figure 5. Effect of $Na_2O/(K_2O+Na_2O)$ ratio on zeolite L crystallization at 443 K. SiO_2/Al_2O_3=30, $(K_2O+Na_2O)/SiO_2$=0.37, $H_2O/(K_2O+Na_2O)$=45, 24hr synthesis.

the reaction mixture was reached to 0.5. However, this increase was not continuous with increasing $Na_2O/(K_2O+Na_2O)$ ratio. In the sodium-richer systems above 0.5 of ratio, further increase of $Na_2O/(K_2O+Na_2O)$ ratio decreased the crystallinity considerably at fixed reaction time of 24h. Cation in synthesis mixture is often the dominant factor determining zeolite structure resulted. Amorphous gels in the composition ranges of $0.4 < Na_2O/(K_2O+Na_2O)$ ratio < 0.6 were converted to the zeolite L phase. For the ratio around 0.5, zeolite L was crystallized as a pure phase with 100% crystallinitywhereas, zeolite W was formed at higher ratio of 0.66. These results obtained in this experiment suggest that a critical molar ratio between K^+ and Na^+ is needed to give pure zeolite L with high crystallinity. Pure zeolite L could be obtained in highly purity at the optimum $Na_2O/(K_2O+Na_2O)$ ratio of around 0.5.

The chemical compositions of the zeolite L samples synthesized with different SiO_2/Al_2O_3 ratios at a constant ratio of $Na_2O/(K_2O+Na_2O)=0.5$ are shown in Table 1. It was found that even though the zeolite L could be synthesized from synthesis mixtures containing Na ions in the ratio of $Na_2O/(K_2O+Na_2O)=0.5$, the cations in the crystal structure of the zeolite L crystals were mostly potassium. This also indicates that the zeolite L structure preferentially incorporates K^+ ions. It is known that K ion is necessary for the crystallization of pure zeolite L, because its framework structure is based on the cancrinite cage occupied by K^+ ion.[15] On the other hand, it was also observed that an increase in the potassium contents of the zeolite L crystals was accompanied with an increase of the aluminum contents, which suggests that the K^+ ions may regulate the initial concentration of aluminum in synthesis mixture. Such dependence as this has been reported by other authors in similar synthesis processes.[16]

Figure 6 shows IR spectrum of the as-synthesized zeolite L synthesized at 443 K. The IR spectrum for zeolite L closely agrees to the literature.[17] Bands near 1160, 1080, and 1015 cm^{-1} correspond to asymmetric stretching modes, and bands near 767 and 721 cm^{-1} are ascribed to a symmetric stretch of internal tetrahedra as well as of external linkages. Bands near 642, 606 and 580 cm^{-1} were assigned to the vibrations of tetrahedra from external linkages of the double rings in the framework structure. Band near 474 cm^{-1} was related to T-O bending mode and a shoulder band around 435 cm^{-1} is characteristic of a pore opening of external linkages.

Table 1. Chemical composition of zeolite L crystals

SiO_2/Al_2O_3 (in gel)	Chemical composition (wt%)				
	Si	Al	K	Na	$Na_2O/(K_2O+Na_2O)$
25	53.59	18.01	16.15	0.50	0.05
28	57.64	18.21	16.22	0.40	0.04
30	57.75	17.39	15.16	0.49	0.05
33	58.15	16.46	14.54	0.52	0.06

Gel composition: $Na_2O/(K_2ONa_2O)0.5$, $(K_2ONa_2O)/SiO_20.37$, $H_2O/(K_2ONa_2O)45$.

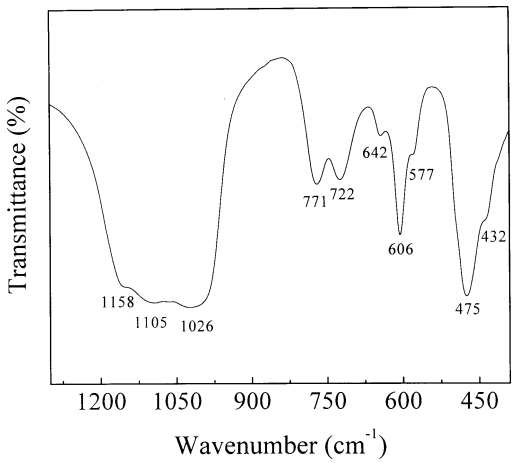

Figure 6. FT-IR spectrum of the as-synthesized zeolite L.

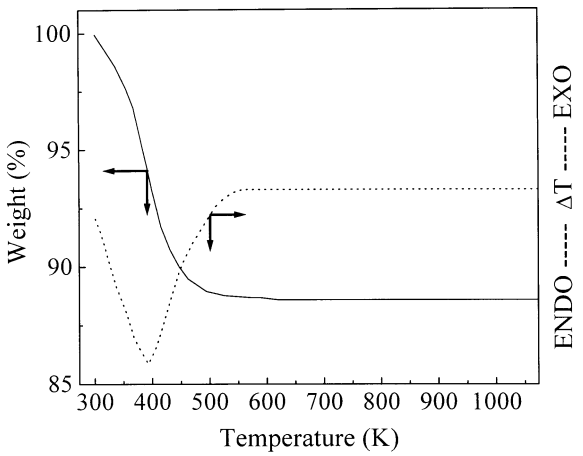

Figure 7. TGDTA thermograms of as-synthesized zeolite L sample.

Thermal stability of the zeolite L obtained was evaluated by a TG/DTA system and the structural changes and the specific surface areas (BET) of the calcined samples at 873-1273 K for 1h were measured by XRD experiment and BET measurement. The thermogravimetric analysis and differential thermogram of the as-synthesized zeolite L are shown in Figure 7. TG/DTA thermograms reveal an endothermic weight loss at 393 K which is characteristic of the zeolite L. The weight loss corresponds to desorption/dehydration of physically sorbed or occluded water. DTA thermogram did not indicate any hightemperature exotherm characteristic of lattice breakdown at least up to 1073 K. This indicates that the zeolite L is structurally stable at least up to 1073 K. Figure 8 shows the specific surface area (BET) and micropore volume of zeolite L calcined at different temperatures. The surface area (BET) of the zeolite L remained almost constant up to 873 K but exhibited a substantial decrease at higher temperatures than 873 K. Especially, it was also found that the specific surface area was decreased substantially around 1073 K. The morphology of zeolite L crystals was, however, still observed in SEM. It is considered that the decrease of

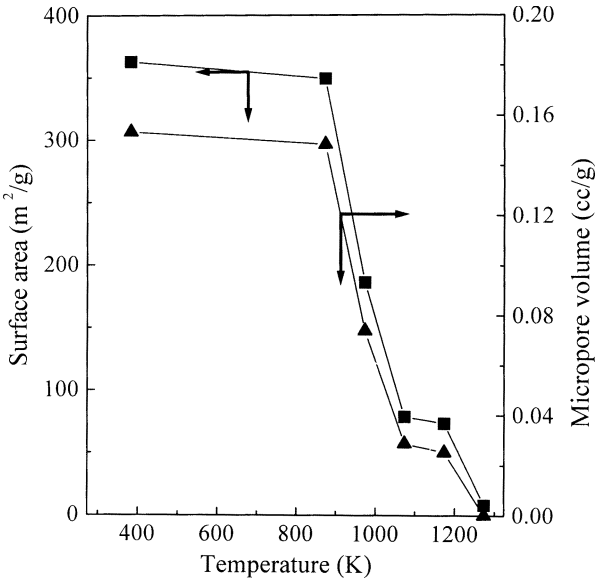

Figure 8. Variation of surface area (BET) and micropore volume of zeolite L samples with different calcination temperatures.

surface areas on calcination above 873 K is due to the loss of micropores as shown in Figure 8. A major part of the surface area is contributed by pores with a diameter characteristic of micropores (less than 2.0 nm). It is believed that the micropore system of zeolite L structure was destroyed by calcination at the temperature above 873 K.

Finally, physico-chemical properties of the zeolite L prepared as a catalyst or as a support were evaluated using the probe reactions of toluene alkylation and n-hexane aromatization. Table 2 shows the catalytic activity and selectivity data of a series of H-form zeolites for toluene alkylation with ethanol at 623 K. As expected, H-ZSM-5(Si/Al27) with medium three-dimensional pores of 5.6×5.4 or 5.1×5.5 Å and a large amount of medium to strong acid sites[18] showed in the highest catalytic activity. The level of conversion approached the thermodynamic equilibrium. Also, H-ZSM-5 had a high selectivity to the formation of ethyltoluene. H-

Table 2. Activity for the alkylation of toluene with ethanol

Catalyst	H-L	H-MOR	H-FER	H-ZSM-5
Conversion (mol%)	9.78	9.6	2.13	44.2
Product distribution (mol%)				
benzene+C_6	1.54	2.19	12.01	5.06
ethylbenzene	1.37	1.48	0.42	2.22
xylene	9.34	10.29	12.72	16.72
ethyltoluene	67.21	64.72	50.32	72.88
trimethyltoluene	11.48	15.84	15.61	2.23
diethyltoluene	9.06	5.48	8.92	1.49
Ethyltoluene isomer selectivity (mol%)				
ortho	29.34	19.81	9.47	3.62
meta	41.08	48.46	53.48	52.42
para	29.58	31.73	37.05	43.96

Reaction condition: temp.: 623K, WHSV=10, toluene/ethanol=2, TOS 2h

Table 3. Products distribution in n-hexane aromatization

Catalyst	Conversion (%)	Selectivity (%)				Benzene yield
		C_1-C_5	C_6 isomer	MCP	C_6H_6	
Pt/KNaL	97	7.0	-	-	93	91
Pt/KL (Tosoh)	91	4.1	0.6	0.3	95	86
Pt/MOR	48	14	-	-	86	41

Reaction conditionstemp. 773 K, atmospheric pressure, H_2/HC6, TOS 0.5h.

L, much the same as H-mordenite, was deactivated quickly after 2h due to one-dimensional pore sturcture being blocked easily by the coke formed at the strong acid sites, despite high catalytic activity at the beginning of the reaction. Concurrently, large 12-membered ring pore structure of the zeolite L (7.1 Å) and mordenite (7.0×6.5 Å) produced relatively high amounts of trimethybenzene or diethylbenzene having large kinetic diameters, and consequently the shape-selectivity to ethyltoluene was diminished. H-ferrierite, having relatively small pores of 3.4×4.4 and 4.3×5.5 Å, resulted in low catalytic activity due to the diffusion limitation of toluene into the catalyst pores.

n-Hexane aromatization reaction was conducted using Pt impregnated (2 wt%) on zeolite L. Product distributions in n-hexane aromatization over Pt loaded zeolite L and mordenite at reaction temperature of 773 K are shown in Table 3. Pt/NaKL catalyst prepared showed a highest conversion of n-hexane and highest selectivity to benzene. It shows sligtly better performance than the commercial Tosoh product. Pt/NaKL is a monofunctional catalyst in which the catalyst acidity plays no role in the reaction and the superior performance of zeolite L to other zeolites structures has been known to be either associated with a tight confinement in the zeolite channel that forces the n-hexane to bend around to promote a ring formation[19] or by providing an environment for highly dispersed Pt clusters.[20] It is interesting to note that mordenite with close structural resemblance to zeolite L produced 50% less benzene yield than with zeolite L. A plausible explanation for this seems that some portion of Pt clusters in mordenites are located at the inaccessible side pocket (2.6×5.7 Å) for n-hexane.

Conclusion

Substantial reduction in synthesis time was achieved for zeolite L crystallization by attempting a hydrothermal synthesis at elevated temperature of 443 K in a Na^+/K^+ mixed alkali system. Highly crystalline zeolite L crystals were obtained in a reproducible manner without zeolite W or T phase impurities at the substrate gel composition of $5.4K_2O$-$5.7Na_2O$-Al_2O_3-$30SiO_2$-$500H_2O$. Zeolite L could be obtained in high purity at the optimum $Na_2O/(K_2O+Na_2O)$ ratio of around 0.5, whilst zeolite W was formed when the $Na_2O/(K_2O+Na_2O)$ ratio was more than 0.66. The chemical analysis of the zeolite L crystals obtained showed that most

potassium hydroxide with a smaller amount of sodium hydroxide was incorporated in the structure regardless of NaOH/KOH used. The zeolite L synthesized was structurally stable up to 1073 K, however, the surface area (BET) of the zeolite L exhibited a substantial decrease at calcination temperatures higher than 873 K. Physico-chemical properties of the zeolite L prepared as a catalyst or as a support were evaluated using the probe reactions of toluene alkylation and n-hexane aromatization. In toluene alkylation, an acid-form H-L catalyst showed the fast deactivation due to one-dimensional pore sturcture being blocked by the coke formed at the strong acid sites, despite high catalytic activity at the beginning of the reaction. In addition, relatively high amounts of trimethybenzene and diethylbenzene were formed due to the large 12-membered ring pore structure of the zeolite L. Pt/NaKL catalyst prepared showed a high conversion of n-hexane and high selectivity to benzene in n-hexane aromatization reaction, far exceeding the performance of Pt/mordenite.

Acknowledgement. This work was carried out with a research fund provided by Inha University.

References

1. Barrer, R. M.; Villiger, H. *Z. Kristallogr* **1969**, *128*, 352.
2. Pichat, P.; Franco Parra, C.; Barthomeuf, D. *J. Chem. Soc. Faraday Trans. I* **1975**, *71*, 99.
3. Breck, D. W.; Acara, N. A. *U.S. Patent* **1965**, *3216*, 789.
4. Nishiimura, Y. *Nippon Kagaku Zasshi* **1970**, *91*, 1046.
5. Tsitsishvilli, G. V.; Krupenikov, A. Y.; Mamulashvili, M. V.; Urushadze, M. V. *Russ. J. Phys. Chem.* **1979**, *53*, 975.
6. Wortel, T. M. *Eur. Pat. Appl.* **1983**, *96*, 479.
7. Vaughan, D. E. W. *Eur. Pat. Appl.* **1985**, *142*, 348.
8. Tsitsishvili, G. V. *Adv. Chem. Ser.* **1973**, *121*, 291.
9. Breck, D. W.; Grose, R. W. *Adv. Chem. Ser.* **1973**, *121*, 319.
10. Rabo, J. A.; Poutsma, M. L. *Adv. Chem. Ser.* **1971**, *102*, 284.
11. Dong, J. L.; Zhu, J. H.; Xu, Q. H. *Appl. Catal. A: General* **1994**, *112*, 105.
12. Tamm, P. W.; Mohr, D. H.; Wilson, C. R. In *Catalysis 1987*; Ward, J. W., Ed.; Elsevier, Amsterdam, **1987**; p 335.
13. Davis, R. J. *Heterogeneous Chemistry Reviews* **1994**, *1*, 41.
14. Bernard, J. R. In *Proceedings of the Fifth International Conference on Zeolites*; Rees, L. V. C., Ed.; Heyden, London, **1980**; p 686.
15. Borowiak, M. A.; Berak, J. M. *Rocz. Chem. Ann. Soc. Chim. Polonorum* **1974**, *48*, 509.
16. Camblor, M. A.; Perez Pariente, J. *Zeolites* **1991**, *11*, 202.
17. Flanigen, E. M.; Khatami, H.; Szymanski, H. A. In *Molecular Sieves Zeolites, Adv. Chem. Ser., 101*; Gould, R. F., Ed.; American Chemical Society: Washington DC., **1971**; p 201.
18. Warren, W.; Kaeding, L.; Brewster, Y.; Chin-Chiun, C. *J. of Catal.* **1984**, *89*, 267.
19. Derouane, E. G.; Vanderveken, D. J. *Appl. Catal.* **1988**, *45*, L15.
20. Iglesia, E.; Baumgarte, J. E. In *New Frontiers in Catalysis*; Guczi, L. *et al*. Eds.; Elsevier: Amsterdam, **1993**; p 993.